ISSN 2070-2051, Protection of Metals and Physical Chemistry of Surfaces, 2018, Vol. 54, No. 5, pp. 834–839. © Pleiades Publishing, Ltd., 2018.
Original Russian Text © I.A. Kirovskaya, E.V. Mironova, A.A. Grigan, O.V. Ushakov, 2018, published in Fizikokhimiya Poverkhnosti i Zashchita Materialov, 2018, Vol. 54, No. 5, pp. 492–498.

NEW SUBSTANCES, MATERIALS AND COATINGS

Comparative Physical-Chemical Properties of Binary and Multicomponent Semiconductors in CdS–ZnSe and CdS–ZnS Systems

I. A. Kirovskaya[a], *, E. V. Mironova[a], A. A. Grigan[a], and O. V. Ushakov[a]
[a] *Omsk State Technical University, Omsk, 644050 Russia*
**e-mail: kirovskaya@omgtu.ru*

Received January 25, 2017

Abstract—Solid substitution solutions in CdS–ZnSe and CdS–ZnS systems have been fabricated and certified. Bulk (crystal chemistry, structural, and optical) and surface (acid–base) properties of these solutions have been examined as compared to each other and their binary components. Regularities of changes in the investigated properties upon changes in the systems' compositions and in a series of analogs have been established: these regularities have predominantly exhibited an extremal nature. Interrelations between the established regularities have been validated, which allows predicting, based only on bulk properties, the surface activity of advanced materials (fabricated solid solutions) toward gases of varied electronic nature—components of natural and technological media. Practical guidelines on application of these materials to produce appropriate sensors have been provided.

Keywords: diamond-like compounds, solid solutions, comparative surface and bulk properties, regularities, prediction, sensors

DOI: 10.1134/S2070205118050118

INTRODUCTION

The unique properties of binary diamond-like compounds, also including those of $A^{II}B^{IV}$ type, as well as the possibilities of controlling and improving bulk and surface properties of corresponding solid solutions, make advanced adsorbents and materials based on these compounds promising for applications in high technologies that incorporate nano- and sensor equipment [1]. To predict these possibilities, it is crucial to establish regularities in the changes of properties along with composition and the correlation between these regularities, not only for this particular system, but also for all parallel systems differing in at least one binary component.

The objective of the present study was to analyze comparative data on bulk (structural, crystal chemistry, and optical) and surface (acid–base) properties of solid solutions in CdS–ZnSe and CdS–ZnS systems and their binary components (CdS, ZnSe, and ZnS).

EXPERIMENTAL

The objects of study comprised primarily finely dispersed powders ($S_{\mathrm{rel}} \leq 1.4$ m^2/g) of CdS, ZnSe, ZnS, and $(\mathrm{CdS})_x(\mathrm{ZnSe})_{1-x}$ ($x = 0.49, 0.55, 0.97$ mol) and $(\mathrm{CdS})_x(\mathrm{ZnS})_{1-x}$ ($x = 0.20, 0.62, 0.78, 0.94$ mol.) solid solutions fabricated by a modified method of isothermal diffusion via a special heating routine [1] and certified mainly on the basis of X-ray data analysis.

X-ray investigation was performed using a D8 Advance diffractometer (Bruker, Germany) under CuK_α irradiation ($\lambda = 0.15406$ nm, $T = 293$ K) via a wide-angle recording technique [2–4] using a Lynxeye position-sensitive detector, as well as a ICDDIPDF-2 database and TOPAS 3.0 software (Bruker, Germany) to decode the obtained X-ray patterns and to determine lattice parameters, respectively.

Electron-microscopic examination was carried out using an SCM-5710 scanning electron microscope equipped by a nitrogen-free X-ray energy-dispersive spectrometer [5].

Optical studies (UV-spectra recording) were performed using spectrophotometers of the type of UV-2501 PC (Shimadzu, Japan) with an ISR-240 A diffusive reflection accessory and SPECORD 40 in the range of 190–900 nm [6]. These measurements were mainly aimed at determining band-gap width ΔE—a crucial semiconductor characteristic—through studying the optical absorption [1].

Absorption coefficient α was calculated from the UV spectra according to the known equation applicable upon multiple radiations passing through a sample:

$$T = (1 - R)^2 e^{-\alpha D} \big/ (1 - R^2 e^{-2\alpha D}),$$

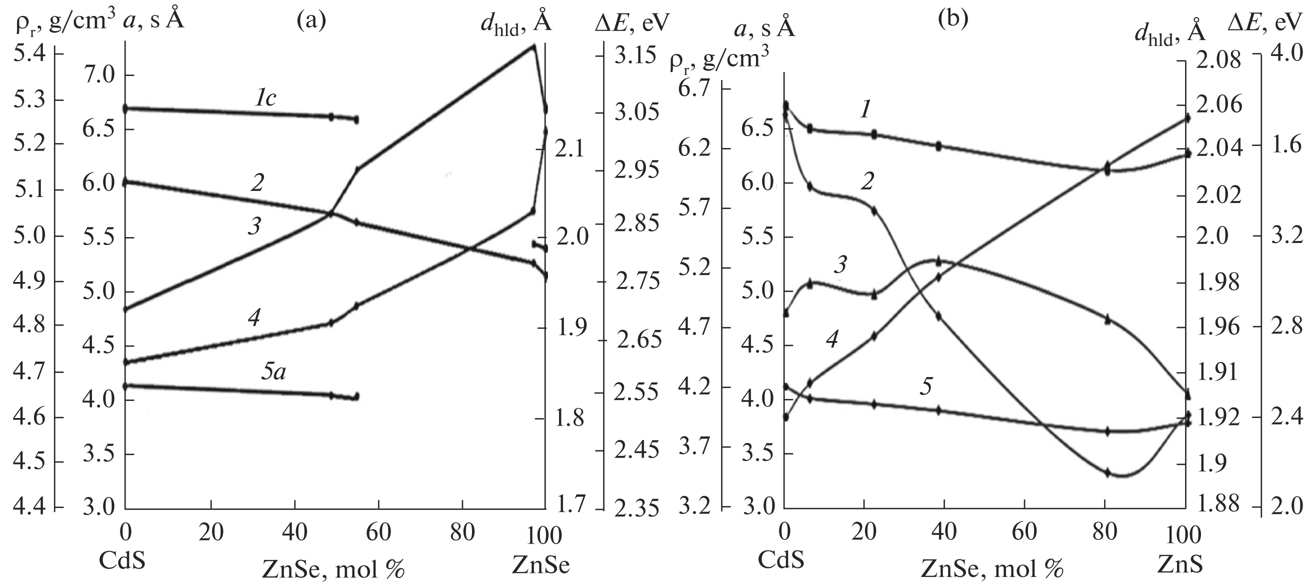

Fig. 1. Dependences on composition of crystal lattice parameters (*5*) *a* and (*1*) *c*, (*2*) interplanar distance d_{110}, (*3*) X-ray density ρ_r, and (*4*) band-gap width ΔE of components of the (a) CdS–ZnSe and (b) CdS–ZnS systems.

where D is the sample thickness, T is the transmission coefficient, and R is the reflection index.

Calculations of α and α^2 were performed using PC custom-designed software.

The $T = f(\lambda)$ and $\alpha^2 = f(h\nu)$ dependences were constructed on the basis of the obtained experimental and calculation data. The band-gap width was determined through extrapolation of the linear section of the $\alpha^2 = f(h\nu)$ dependence until the point of intersection with the $h\nu$ axis [1].

Surface activity was estimated from pH value of the surface isoelectric state $\mathrm{pH_{iso}}$ and total concentration of acidic sites C_{total}. $\mathrm{pH_{iso}}$ values were obtained by the hydrolytic adsorption method with an introduction of ampholyte adsorbents represented by CdS, ZnSe, and ZnS and $(\mathrm{CdS})_x(\mathrm{ZnSe})_{1-x}$ and $(\mathrm{CdS})_x(\mathrm{ZnS})_{1-x}$ solid solutions with typical isoelectric points corresponding to the solubility minimum. The final task consisted in detecting the medium pH at which ampholyte adsorbents were able to detach equal (very small) amounts of $\mathrm{H^+}$ and $\mathrm{OH^-}$ ions [7].

Having data on the $\mathrm{pH_{iso}}$ values would enable one to determine the average power and ratio of acid and base sites.

To determine C_{tot}, the nonaqueous conductometry titration method was used [1]. In this case, the electric conductivity of an equilibrium mixture (dispersed adsorbent–semiconductor + solvent (methyl ethyl ketone)) was measured with an introduction of titrant (potassium ethylate). Based on the constructed differential curves, dependences of the specific conductivity on the titrant volume, and the concentration of acidic sites (total and for individual peaks) were calculated according to the formula

$$\mathrm{C} = VN \times 1000/m,$$

where V is the volume of potassium ethylate spent in titration, mL; N is the normal concentration of potassium ethylate solution, g-eq/L; and m is the weight of adsorbent, g.

The reproducibility and the accuracy of the experimental data were verified by parallel measurements using the methods of mathematical statistics and quantitative analysis data processing. Statistical processing of the obtained values, calculations of measurements errors, and building and processing of graphic dependences were performed using the Stat-2, Microsoft Excel, and Origin software.

RESULTS AND DISCUSSION

According to the X-ray data (relative positioning and distribution of the main lines on X-ray images of binary components and solid solutions [1], found values of crystal lattice parameters a and c, interplanar distances d_{hkl}, and density ρ_r) (Fig. 1), solid substitution solutions were formed in the systems under study. The solutions exhibited a cubic sphalerite structure (at $x_{\mathrm{CdS}} \leq 0.03$ mol) and a hexagonal wurtzite structure (at $x_{\mathrm{CdS}} \geq 0.45$ mol) in the CdS–ZnSe system and a hexagonal wurtzite structure in the CdS–ZnS system.

That formation of solid substitution solutions had occurred was indirectly corroborated by a certain regularity in the UV spectra relative positioning (Fig. 2) and, correspondingly, virtually linear or smoothly changing of the band-gap width ΔE along with

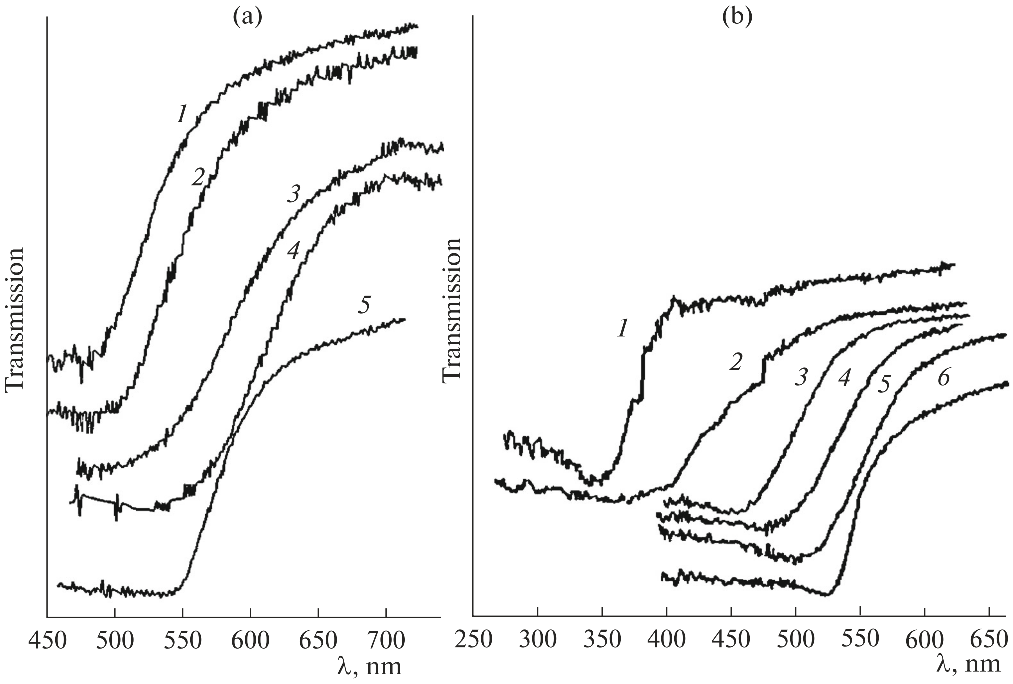

Fig. 2. UV spectra of components of the (a) CdS–ZnSe system ((*1*) ZnSe, (*2*) $(CdS)_{0.03}(ZnSe)_{0.97}$, (*3*) $(CdS)_{0.45}(ZnSe)_{0.55}$, (*4*) $(CdS)_{0.51}(ZnSe)_{0.49}$, and (*5*) CdS) and (b) the CdS–ZnS system ((*1*) ZnS, (*2*) $CdS_{0.20}ZnS_{0.80}$, (*3*) $CdS_{0.62}ZnS_{0.38}$, (*4*) $CdS_{0.78}ZnS_{0.22}$, (*5*) $CdS_{0.94}ZnS_{0.06}$, and (*6*); CdS).

changes in the composition (Fig. 1). The latter, just like in changes of a, c, and d_{hkl} along with the composition, indicated a prevalence of the statistical factor as opposed to the extremal pattern observed for X-ray density ρ_r changes (Fig. 1).

Its acceptability was demonstrated in [1, 8, 9], where corresponding generalizations and explanations were provided based on a detailed analysis of semiconductor solid solutions investigation data.

The element composition of solid solutions and the binary systems components that conformed satisfactorily to the molar composition, the average sizes and numbers of the most represented particles, and their dependences on the systems' composition were determined *based on electron microscopy data* [10, 11]. The polycrystalline structure of the surface with inhomogeneously distributed crystallites able to associate into agglomerates, including grains of varied size, was established.

Let us examine surface-active (acid–base) properties of CdS–ZnSe and CdS–ZnS system components. pH values of the isoelectric state of these systems' surfaces exposed to air in the series

$$CdS \rightarrow (CdS)_x(ZnSe)_{1-x} \rightarrow ZnSe,$$

$$CdS \rightarrow (CdS)_x(ZnS)_{1-x} \rightarrow ZnS$$

fit within the ranges of 6.4–8.2 and 6.4–6.86, respectively, which indicated a predominantly basic surface nature of zinc selenide and $(CdS)_x(ZnSe)_{1-x}$ solid solutions and weakly acidic surface nature of CdS–ZnS system components.

These properties changed in an extremal manner upon changes in the compositions of CdS–ZnSe and CdS–ZnS systems: through a minimum at an excess of ZnSe in the first case and through maxima at excesses of ZnS and CdS in the second case (Fig. 3).

Results of nonaqueous conductometry titration demonstrated different types of acidic sites on the initial (exposed to air) surfaces of the CdS–ZnSe and CdS–ZnS systems' surfaces, with curves $\Delta\sigma/\Delta V$–V containing three or four peaks (Fig. 4).

As we have stated earlier (for example, [1, 9]), coordination-unsaturated atoms (Lewis sites), as well as adsorbed water molecules and OH^- groups (Brønsted sites), can act as acidic sites.

Both of the above may be determinative in the investigated cases. For example, Lewis sites—coordination-unsaturated atoms with varied levels of unsaturation and, consequently, varied effective charges (q_{ef})—must make a predominant contribution to the acid–base state of the surface of the CdS–ZnS system components characterized with $pH_{iso} < 7$, which was corroborated by the formation of donor–acceptor complexes with their participation, for example, $NH_3^{+\delta}$–$A^{-\delta}$ (A—Cd, Zn), demonstrated by IR spectra,

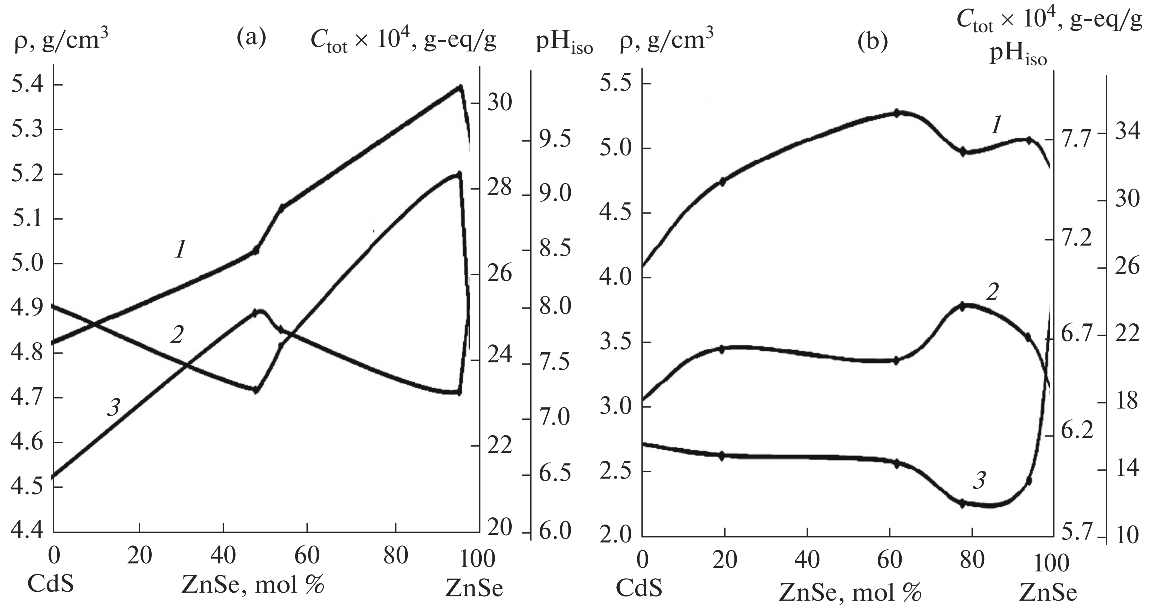

Fig. 3. (*1*) Dependences of X-ray density ρ_r, (*2*) pH-isoelectric surface state pH$_{iso}$, (*3*) and total acidic site concentration C_{tot} and values of components of (a) CdS–ZnSe and (b) CdS–ZnS on composition.

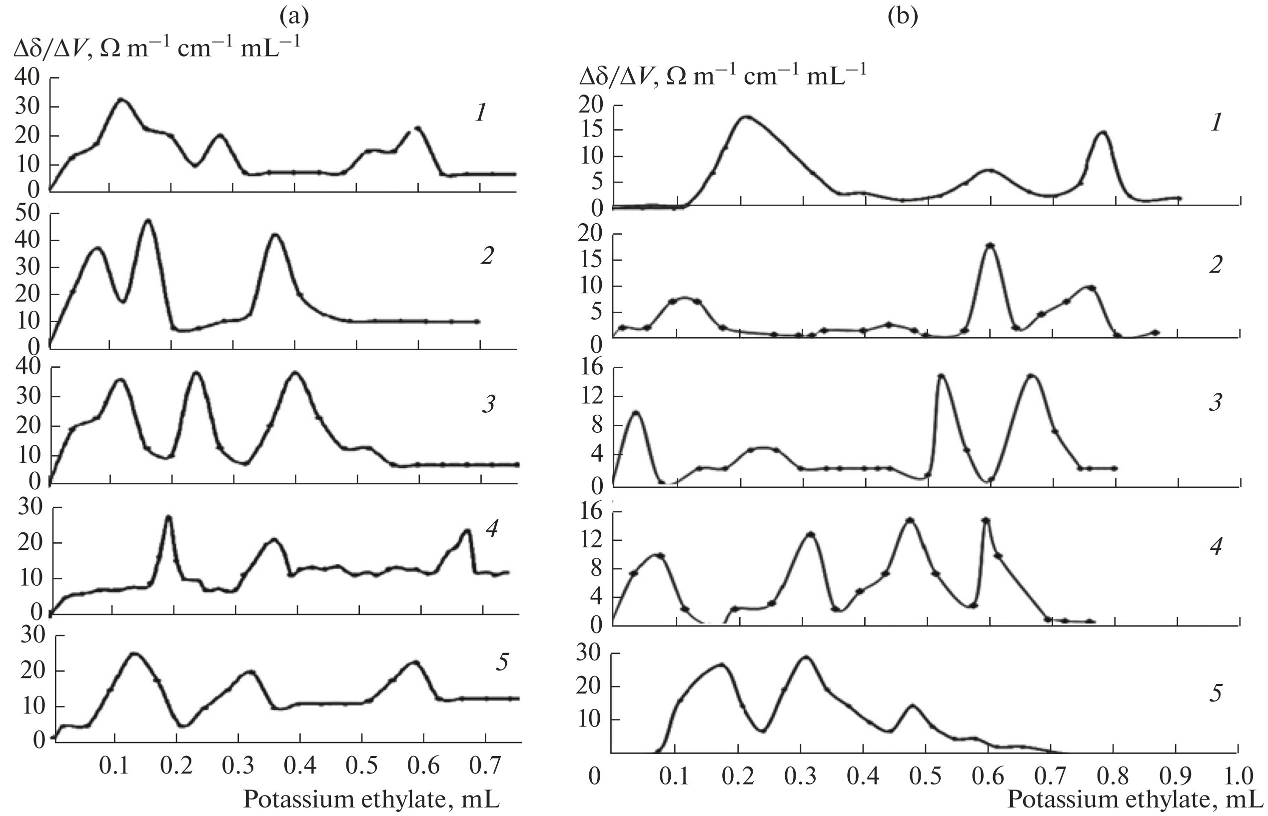

Fig. 4. Differential curves of nonaqueous conductometry titration of the components exposed in air of (a) the CdS–ZnSe system ((*1*) ZnSe, (*2*) $(CdS)_{0.03}(ZnSe)_{0.97}$, (*3*) $(CdS)_{0.45}(ZnSe)_{0.55}$, (*4*) $(CdS)_{0.51}(ZnSe)_{0.49}$, and (*5*) CdS) and (b) the CdS–ZnS system ((*1*) ZnS, (*2*) $CdS_{0.20}ZnS_{0.80}$, (*3*) $CdS_{0.62}ZnS_{0.38}$, (*4*) $CdS_{0.78}ZnS_{0.22}$, (*5*) $CdS_{0.94}ZnS_{0.06}$, and (*6*) CdS).

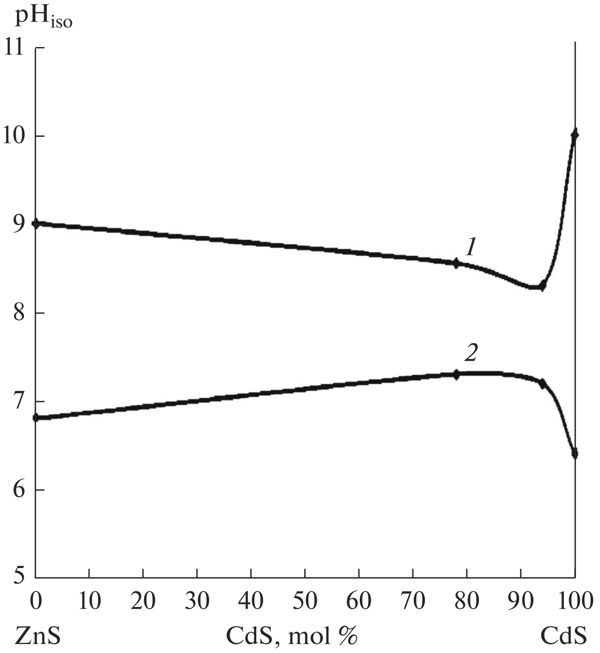

Fig. 5. Dependences of pH values of isoelectric state of components of the ZnS–CdS system exposed to argon (*2*) and NH$_3$ (*1*) treatment.

as well as by a nature of the influence of the principal gas (NH$_3$) on pH$_{iso}$ (an increase was observed) (Fig. 5).

Brønsted sites must make a predominant contribution to the acid–base state of the surface of the CdS–ZnS system components at pH$_{iso}$ > 7. This was indicated by an elevated activity of these surfaces toward acidic gases found from the results of direct adsorption investigation. In particular, $\alpha_{CO_2}/\alpha_{NH_3} > 1$ even considering the reversible character of adsorption of ammonia (i.e., at a weak adsorption bond) (for example, see Fig. 6).

Comparing the dependences of the investigated properties on composition within each of the CdS–ZnSe and CdS–ZnS systems was of interest, as was examining similar dependences of the various indicated systems taking into account changes in the corresponding physical-chemical properties in a series of analogs—the initial binary components of these systems: CdS → ZnSe → ZnS. *As a result, the following interrelated regularities were identified.*

The CdS–ZnSe system with an increase in ZnSe concentration (wide-band-gap component) demonstrated a decrease in interplanar distance d$_{hkl}$ and crystal lattice parameters *a* and *c* and extremal changes (at an excess of ZnSe) of X-ray density ρ_r, pH$_{iso}$, and C_{tot} (Figs. 1, 3a). The presence of both direct and inverse relations between ρ_r and pH$_{iso}$ is worth mentioning. The direct relation was determined from the decrease of coordination–unsaturation of atoms both in the bulk and on the surface with an increase in ρ_r increase and corresponding increase in the density of their packing per volume unit of the crystal lattice. Hence, the decrease of the Lewis sites' contribution determining the surface acidity and the increase of that of Brønsted sites that resulted in pH$_{iso}$ increase toward CdS → $(CdS)_x(ZnSe)_{1-x}$ → ZnSe.

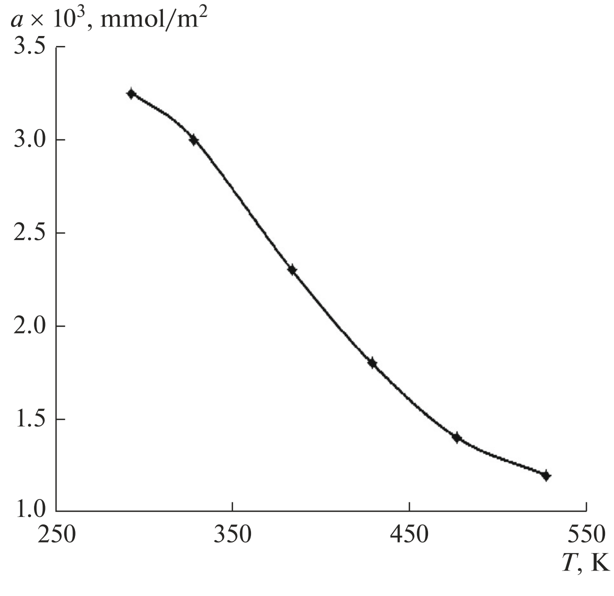

Fig. 6. Isobar of adsorption isobar of ammonia on zinc selenide at $P_N = 56$ Pa.

Here, at an excess of zinc selenide ($x_{ZnSe} = 0.97$ mol.), the atomic packing density in the bulk increases so much and their connection to surface atoms loosens so much that an explosion of the surface atoms' coordination–unsaturation is observed, which is followed by a decrease by pH$_{iso}$ (Fig. 3a). It is worth noting that other compositions of the CdS–ZnSe system also demonstrated a predominant effect of the zinc selenide (the second binary component) on the surface acid–base state, exhibiting a wider band-gap width than the first binary component (CdS) ($\Delta E_{ZnSe} = 2.7$–2.9 eV, $\Delta E_{CdS} = 2.42$ eV).

Under a predominantly basic nature of the surface of the CdS–ZnSe system, the components have been hypothesized to manifest an elevated activity toward acidic gases, which was corroborated by the above data.

The discovered regularities of changes in volume and surface properties with the composition of the *CdS–ZnS* system, except for $(a, c) = f(x_{CdS})$ and $\Delta E = f(x_{CdS})$, exhibited an extremal nature (Figs. 1, 3b), which, as we stated earlier, was to a great extent determined by the complex inner processes that followed the formation of solid solutions. Here, it is worth mentioning an inverse positioning of extrema on the pH$_{iso} = f(x_{CdS})$ and $C_{tot} = f(x_{CdS})$ and pH$_{iso} = f(x_{CdS})$ and $\rho_r = f(x_{CdS})$ curves (Fig. 3b): the minimum and maximum on the $pH_{iso} = f(x_{CdS})$ curve corresponded to the maxima and minima on the $C_{tot} = f(x_{CdS})$ and $\rho_r = f(x_{CdS})$ curves. Thus, a relationship was observed between density ρ_r, the relative contribution of coordination-unsaturated atoms (Lewis sites), and the surface acidity.

In addition, it was of interest to observe the "behavior" of the investigated physical-chemical properties in the series of analogues CdS → ZnSe → ZnS—the initial binary components of the CdS–ZnSe and CdS–ZnS systems.

Note that, upon a transition from CdS to ZnS, they changed through extrema corresponding to ZnSe (Fig. 7). The latter was reflected in the physical-chemical properties of solid solutions, in particular, those of the CdS–ZnSe system (Figs. 1, 3a). The CdS–ZnS system demonstrated the effect of both excess binary components (Fig. 3b).

Aside from the obvious academic interest, the identified interrelations between surface and bulk physical-chemical properties (Figs. 1, 3) also open up possibilities of preliminarily selecting optimal materials for equipment (sensors, in our case) based only on the data of bulk physical-chemical properties (X-ray density ρ_r in particular), skipping not only laborious adsorption investigations, but also determination of acid–base properties.

Since the CdS–ZnSe system components, except for CdS, exhibited primarily a basic surface and the CdS–ZnS components primarily acidic ones, they can be recommended, respectively, for production of sensors on microimpurities of acid (NO_2, SO_2 types) and base (NH_3 type) gases [9].

CONCLUSIONS

Solid solutions in the CdS–ZnSe and CdS–ZnS systems verified as being solid substitution solutions have been fabricated: they exhibited (depending on the composition) a cubic sphalerite structure and a hexagonal wurtzite structure in the CdS–ZnSe system and a hexagonal wurtzite structure in the CdS–ZnS system. A crucial parameter of semiconductor materials (solid solutions)—high-energy gap width (ΔE) values—have been determined from the UV-spectra for the first time.

Bulk (crystal chemistry, structural, and optical) and surface (acid–base) properties of the fabricated solid solutions and the initial binary components (CdS, ZnSe, ZnS) have been examined. Regularities of changes in the investigated properties with those of the CdS–ZnSe and CdS–ZnS systems have been established.

A certain parallel has been drawn between the nature of the properties changes with compositions of CdS–ZnSe and CdS–ZnS systems and in a series of analogues—the initial binary components of these systems, CdS → ZnSe → ZnS—from the suggested point on the nature of active sites.

The identified interrelations between the established regularities have been confirmed, which enables one to predict the surface activity of new materials with respect to gases of differing electron nature (components of natural and technological media) on the basis of only bulk properties.

The fabricated solid solutions are recommended for production of sensors for acidic ($pH_{iso} > 7$) or basic ($pH_{iso} < 7$) gases.

ACKNOWLEDGMENTS

The present study was performed within the framework of a state assignment of the Ministry of Education and Science of the Russian Federation. no. 4.2543.2014/K.

REFERENCES

1. Kirovskaya, I.A., *Tverdye rastvory binarnykh i mnogokomponentnykh poluprovodnikovykh sistem* (Solid Solutions of Binary and Multicomponent Semiconductor Systems), Omsk: Omsk State Technical Univ., 2010.
2. Mirkin, S.E., *Spravochnik po rentgenostrukturnomu analizu* (X-Ray Structural Analysis. Handbook), Moscow: Gosudarstvennoe Izd. Fiziko-Matematicheskoi Literatury, 1961.
3. Gorelik, S.S., Rastorguev, L.N., and Skakov, Yu.A., *Rentgenograficheskii i elektronnoopticheskii analiz* (X-Ray and Electron-Optical Analysis), Moscow: Metallurgiya, 1970.
4. Smyslov, E.F., *Zavod. Lab., Diagn. Mater.,* 2006, vol. 72, no. 5, p. 33.
5. Goldstein, J.I., Williams, D.B., and Lyman, C.E., *Ultramicroscopy,* 1989, vol. 28, p. 56.
6. Kosyachenko, L.A., Sklyarchuk, V.M., Sklyarchuk, O.V., and O. L. Maslyanchuk, *Semiconductors,* 2011, vol. 45, no. 10, p. 1273.
7. Maidanovskaya, L.G., *Kataliticheskie reaktsii v zhidkoi faze* (Catalytic Reactions in Fluid Phase), Alma-Ata: Acad. Sci. Kazakh SSR, 1963, p. 212.
8. Kirovskaya, I.A., *Zh. Fiz. Khim.,* 1985, vol. 59, no. 1, p. 1323.
9. Kirovskaya, I.A., *Fiziko-khimicheskie svoistva binarnykh i mnogokomponentnykh almazopodobnykh poluprovodnikov* (Physical and Chemical Properties of Binary and Multicomponent Diamond-Like Semiconductors), Novosibirsk: Siberian Branch Russ. Acad. Sci., 2015.
10. Kirovskaya, I.A., Mironova, E.V., Ushakov O.V., et al., *Procedia Eng.,* 2016, vol. 152, p. 681.
11. Kirovskaya, I.A., Mironova, E.V., Grigan, A.A., et al., *Omsk. Nauchn. Vestn.,* 2016, no. 1, p. 69.

Translated by D. Marinin